Journal of Macromolecular Science, Part A
Publication details, including instructions for authors and subscription information:
http://www.informaworld.com/smpp/title~content=t713597274

POLYIMIDE/INORGANIC INTERPENETRATING POLYMER NETWORKS FOR STABLE SECOND-ORDER NONLINEAR OPTICS

Ru-Jong Jeng[a]; Li-Hsin Chan[a]; Rong-Ho Lee[b]; Ging-Ho Hsiue[a]; Huey-Ling Chang[c]
[a] Department of Chemical Engineering, National Chung Hsing University, Taiwan, ROC [b] Opto-Electronics & Systems Laboratory, Industrial Technology Research Institute, Taiwan, ROC [c] Department of Chemical Engineering, National Chinyi Institute of Technology, Taiwan, ROC

Online publication date: 30 November 2001

To cite this Article Jeng, Ru-Jong , Chan, Li-Hsin , Lee, Rong-Ho , Hsiue, Ging-Ho and Chang, Huey-Ling(2001) 'POLYIMIDE/INORGANIC INTERPENETRATING POLYMER NETWORKS FOR STABLE SECOND-ORDER NONLINEAR OPTICS', Journal of Macromolecular Science, Part A, 38: 12, 1259 — 1274
To link to this Article: DOI: 10.1081/MA-100108382
URL: http://dx.doi.org/10.1081/MA-100108382

J. MACROMOL. SCI.—PURE APPL. CHEM., A38(12), 1259–1274 (2001)

POLYIMIDE/INORGANIC INTERPENETRATING POLYMER NETWORKS FOR STABLE SECOND-ORDER NONLINEAR OPTICS

Ru-Jong Jeng,[1,*] Li-Hsin Chan,[1] Rong-Ho Lee,[2] Ging-Ho Hsiue,[1] and Huey-Ling Chang[3]

[1]Department of Chemical Engineering, National Chung Hsing University, Taichung 402, Taiwan, ROC
[2]Opto-Electronics & Systems Laboratory, Industrial Technology Research Institute, Chutung, Hsinchu 310, Taiwan, ROC
[3]Department of Chemical Engineering, National Chinyi Institute of Technology, Taichung 411, Taiwan, ROC

Dedicated to the memory of Professor Sukant K. Tripathy.

ABSTRACT

Thermally stable NLO interpenetrating polymer networks (IPNs) based on an organosoluble polyimides functionalized with methacryloyl groups (PIB), and an alkoxysilane dye (ASD) have been developed. IPNs were formed through the free radical polymerization of methacryloyl group containing PIB, and sol-gel process of ASD. Optically clear samples exhibit large second-order optical nonlinearity (d_{33} = 6.9-39.6 pm/V at 1064 nm) after poling and curing at 180°C for 2 hours. The temporal stability of the PIB/ASD IPN samples was much better than the inter-chain crosslinking polyimide/inorganic samples. The high rigidity of the polymer backbone and the interpenetrating structure of the polymer networks prevent the randomization of the aligned NLO chromophores.

Key Words: Nonlinear optics; Polyimide; Sol-gel process; IPN

*Corresponding author.

INTRODUCTION

There has been tremendous interest in the second-order nonlinear optical (NLO) polymeric materials for their potential use in electrooptic applications [1-2]. However, the major drawback of NLO polymers that prevents them from being employed in device applications is the decay of their electric field induced second-order optical nonlinearities [3-9]. The decay is caused by the relaxation of the NLO chromophores from the induced non-centrosymmetric alignment to a random fashion. Numerous efforts have been made to enhance the stability and processability of NLO materials based on polyimides. They are guest-host system, side chain type, and crosslinked type NLO polyimides [10-14].

NLO sol-gel materials with low temperature processing capability, excellent optical quality and thermal stability, refractive index control of films, and ease of device fabrication are promising for applications in photonic devices [15-18]. Organically modified inorganic NLO sol-gel materials are obtained via incorporation of the organic NLO-active chromophore into alkoxysilane-based inorganic network. The formation of three-dimensional silicon oxide networks via sol-gel process would prevent the randomization of poled NLO chromophores in the absence of a poling field. Tripathy *et al.* reported a second-order NLO organic/inorganic composite based on an alkoxysilane dye and an aromatic polyimide [12]. Polyimide films containing a homogeneous dispersion of SiO_2 particles have been achieved through a sol-gel process. The incorporation of an inorganic sol-gel material provides an inert environment for the polyimide and theoretically will prevent its thermal decomposition. The inorganic networks will be densely and uniformly packed throughout the organic chain segments by the sol-gel process [19]. The interactions between an inorganic oxide and polyimide will reduce the molecular motions during the glass transition [19]. Therefore, the incorporation of an inorganic NLO sol-gel material within an organic polyimide is a reasonable approach to enhance long-term NLO stability.

Recently, we have reported an organic-inorganic NLO material based on the organosoluble polyimide A (PIA; Figure 1(a)) and an alkoxysilane dye (ASD; Figure 1(c)) via sol-gel process [20]. In addition to a sol-gel reaction among ASDs, the methoxyl groups of ASD were reacted with the aromatic hydroxyl groups of PIA to form crosslinked NLO-active polyimide via phenoxysilicon linkages [14]. Excellent temporal stability was obtained for these poled/cured PIA/ASD samples. To further enhance the temporal stability, a series of an organosoluble polyimide B (PIB; Figure 1(b)) and an alkoxysilane dye (ASD) based interpenetrating polymer networks (IPNs) were developed in this investigation. The IPN is known to be able to remarkably suppress the creep and flow phenomena in polymers, and to promote compatibility between two polymers via simultaneous polymerization reactions [21]. The molecular motion of each polymer in IPN is restricted due to the entanglements between different networks. Thus, the introduction of a crosslinkable high T_g polyimide into an IPN structure is expected to further advance the T_g of the system and boost the stability of the

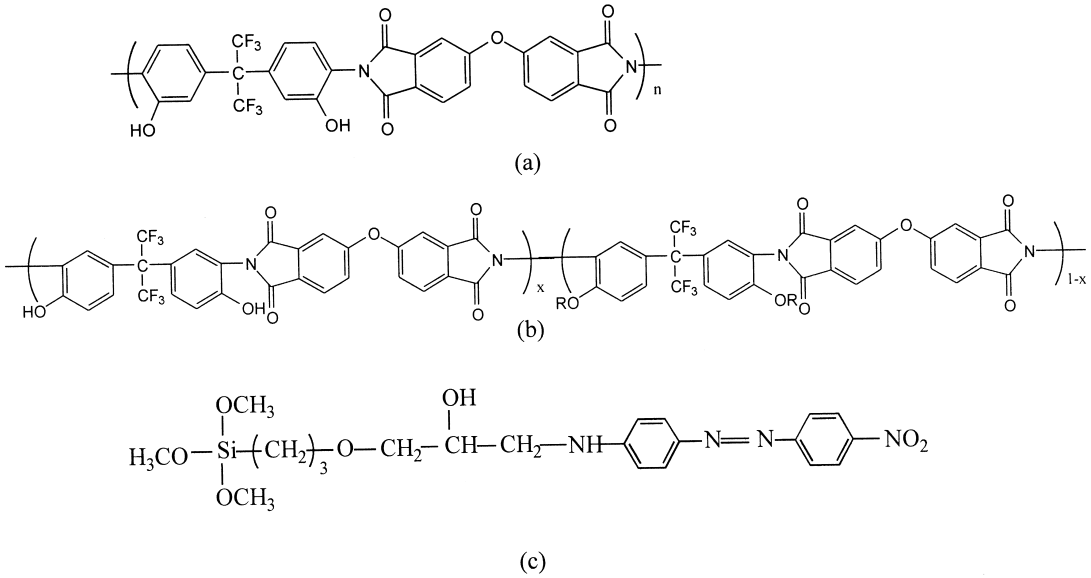

Figure 1. Chemical structures of the (a) PIA, (b) PIB, and (c) ASD.

nonlinearity of the IPN [21]. Thermal behaviors of these organic-inorganic NLO IPNs were studied with DSC and TGA, respectively. Phase homogeneity was analyzed using scanning electron microscopy (SEM). Furthermore, the composition effect on the temporal stability and relaxation behavior of the NLO property were studied in detail.

EXPERIMENTAL

The organosoluble polyimide, PIA was successfully synthesized by a solution imidization technique [22]. PIB was synthesized by the reaction of PIA and methacryloyl chloride in tetrahydrofuran (THF) with suitable amount of 1-methyl-2-pyrrolidinone (NMP) and triethylamine (TEA) as catalysts. The polyimide was separated and purified by several re-precipitations from THF solution into methanol, and then dried under vacuum. The chemical structure of PIB was characterized by using the ^{1}H-NMR spectroscopy (Brüker AMX400). The alkoxysilane dye (ASD) was synthesized by the coupling of a monoepoxy of (3-glycidoxypropyl) trimethoxysilane and a monoamine of 4-[(4'-nitrophenyl)azo] phenylamine (Disperse Orange 3) [23]. The reactions of these NLO materials were characterized by the Fourier transform infrared (FTIR) spectroscopy (Bio-Rad FTS155 FTIR). T_g's were determined using differential scanning calorimetry (DSC; Seiko SSC/5200) at a heating rate of 10°C/min. Degradation temperature (T_d) was measured on a Seiko Exstar 6000 thermogravimetric analyzer (TGA) at 10°C/min under air. UV-vis spectra were recorded on a Perkin Elmer Lambda 2S

spectrophotometer. SEM (Jeol JEM-840A) was used to study the morphology of the polymer film (gold coated).

The compositions of PIB and ASD in different weight ratios (10/90, 30/70, 50/50, 70/30, 90/10 wt%) were respectively dissolved in the THF with the addition of 10 mg of 90% methanoic acid to aid the hydrolysis of ASD. The polymer solution was stirred at room temperature for 3 hours. Thin films were prepared by spin-coating the polymer solution onto indium tin oxide (ITO) glass substrates. The poling process for the second-order NLO polymer films was carried out using an *in situ* poling technique. The details of the corona poling set-up were the same as was reported earlier [24]. The poling process was started at room temperature and increased to 180°C at heating rate of 15°C/min. The corona current was maintained under 4 μA with a potential of 5.5 kV while the poling temperature was kept at 180°C for 2 hours. The formation of the network and the molecular alignment of the poled order proceeded simultaneously during this period. Upon saturation of the SHG signal intensity, the sample was then cooled down to room temperature in the presence of the poling field at which point the poling field was terminated. Thickness and indices of refraction were evaluated by a prism coupler (Metricon 2010). Second harmonic generation measurements were carried out with a Q-switched Nd:YAG laser operating at 1064 nm. Measurement of the second harmonic coefficient, d_{33}, has been previously discussed [25], and the d_{33} values were corrected for absorption [26].

RESULTS AND DISCUSSION

^{1}H-NMR spectrum of the methacryloyl group containing PIB is shown in Figure 2. The resonance peaks of protons have been identified for PIB. The resonance peaks of protons g and h appear at $\delta = 5.23$ and $\delta = 5.9$-6.1. Moreover, the proton i shows up at $\delta = 9.5$. From the integration of peak areas of protons h and i, the methacryloyl group content was obtained for the PIB. It was found that the extent of functionalization of t methacryloyl groups was more than 90 mol% for the PIB sample. In addition to the ^{1}H-NMR spectrum, the chemical structure of PIB was also characterized by the FTIR. The FTIR spectrum of PIB is shown in Figure 3(a). The absorption peaks of the imide group were observed at 1720 and 1780 cm^{-1}. Moreover, the absorption intensity of the hydroxyl group at 3400 cm^{-1} was decreased remarkably due to the functionalization of the methacryloyl groups on the polymer chains of PIB. The absorption peak of vinyl group in methacryloyl group was observed at 1700 cm^{-1}.

For the PIB/ASD samples, the IPN structure was formed simultaneously when the polymer film was heated at elevated temperatures. The PIB based organic network was formed through the free radical polymerization of the methacryloyl groups, whereas the inorganic network of ASD was obtained via the sol-gel process. The curing conditions were determined using DSC reaction scan. The optimum curing condition of polyimide/ASD samples was chosen to be at

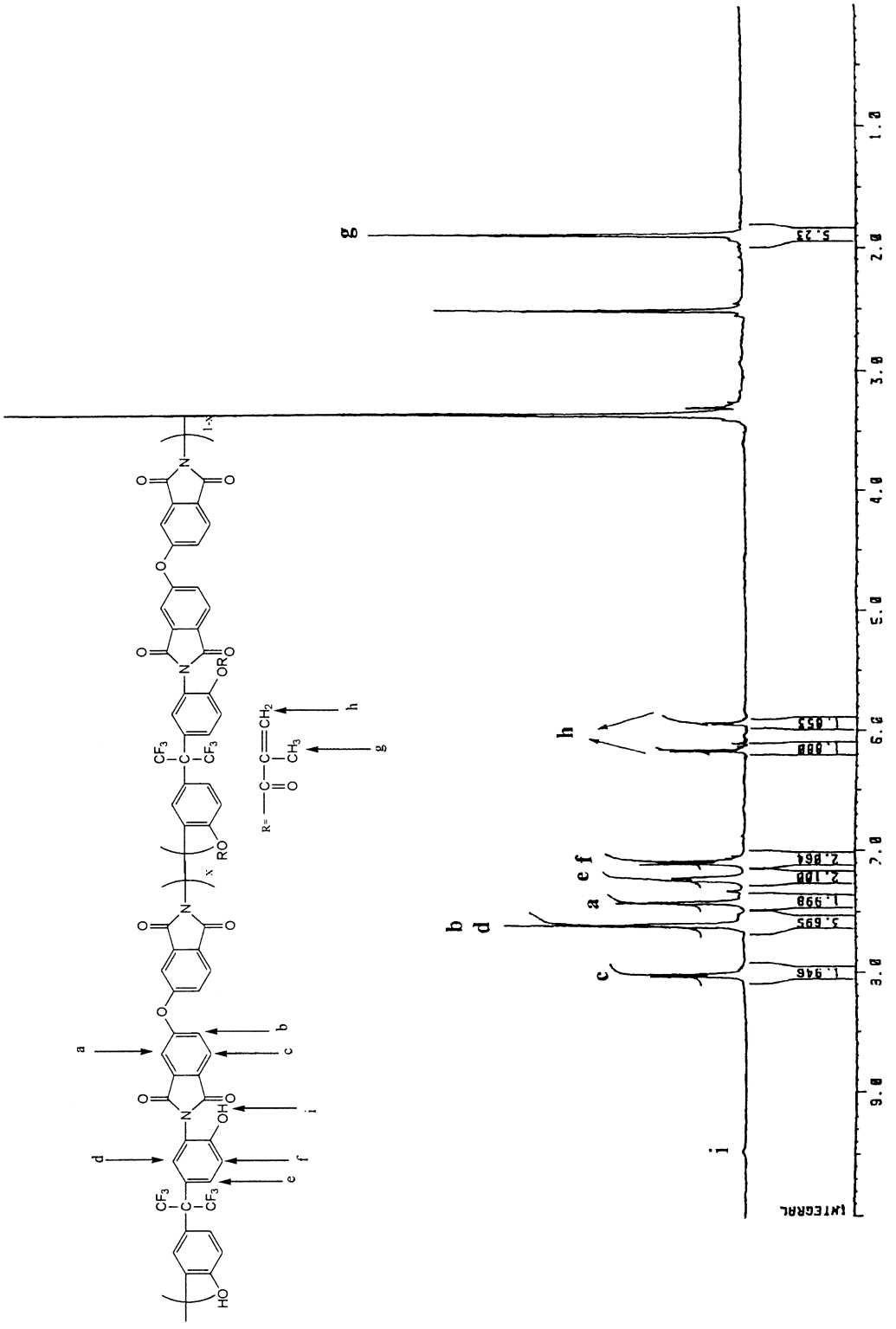

Figure 2. ^{1}H-NMR (DMSO-d_6) spectrum of the PIB sample.

180°C for 2 hours due to the consideration of the thermal stability of ASD, and effective alignment of the NLO chromophores. Figure 3 also shows the FTIR spectra of the PIB50 and cured PIB50 (PIB:ASD = 50:50 by weight) samples. The free radical polymerization of the methacryloyl groups results in the disappearance of the ethylene absorption peak at 1700 cm^{-1} for the cured PIB50 sample. The broadening absorption peak at around 1100 cm^{-1} was identified as the formation of Si-O-Si linkages resulted from sol-gel reaction among ASDs [12]. The FTIR results demonstrated the respective reactions of the PIB and ASD proceeded simultaneously during the optimum curing process.

T_g's of the polyimides are shown in Figure 4. T_g's of PIA was observed at temperature of 230°C. For the cured PIB sample, a broad glass transition was vaguely observed at temperatures around 300°C. However, T_g's were not detectable from the DSC study for the PIB/ASD IPN samples because of the formation of high crosslinking density of the organic and inorganic networks [20]. Thermal decomposition behavior of the PIB/ASD samples was measured on a TGA under air after curing at 180°C for 2 hours. T_d was read at the temperature corresponding to the weight loss of 5%. The compositions and T_d's of the PIB and PIB/ASD IPN samples are summarized in Table 1. T_d was observed at temperature above 349°C for the PIB. Moreover, T_d's of the PIB/ASD samples were observed in the range of 272 to 293°C. It is important to note that the 5% wt. loss of the NLO materials mostly results from either further sol-gel reaction (i.e., condensation) of residual silanol groups [27], or degradation of the NLO moieties (i.e., azobenzene). The decomposition rate was decreased with increasing PIB content in the range of 300

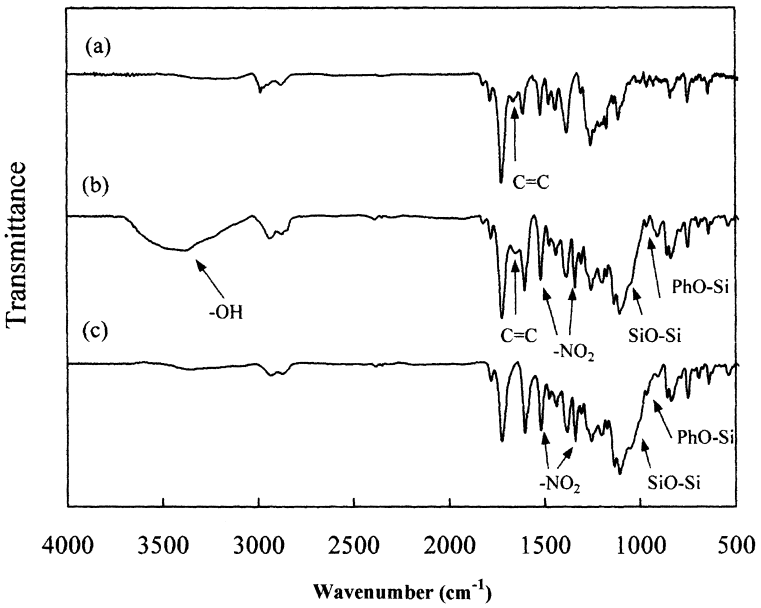

Figure 3. Infrared spectra of the (a) PIB, (b) PIB50, and (c) cured PIB50 samples.

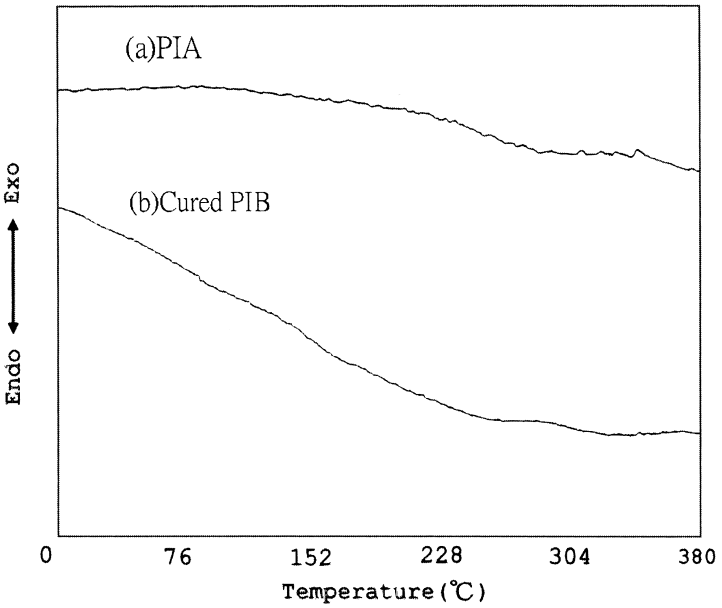

Figure 4. DSC thermograms of the PIA and cured PIB samples.

to 550°C due to the high T_d of PIB. Moreover, a higher silicon-containing ASD content led to a higher char yield for the PIB/ASD IPN sample at temperatures above 600°C. Moreover, the cured PIB/ASD samples exhibited much higher T_d's than that of the cured ASD (T_d = 247). Thermal decomposition behavior of the PIB/ASD samples was similar to that of the cured PIA/ASD samples [20].

The homogeneity of the PIB/ASD samples was studied using SEM. The fractured surfaces of the cured PIB90, PIB50 and PIB10 are shown in Figure 5. No sign of phase separation was observed when magnification was increased up to 5 K. In addition, the distribution of inorganic networks in the polymer matrix was investigated using SEM with a mapping technique. The mapping spectra of the PIB90, PIB50 and PIB10 IPN samples are shown in Figure 6. The results indi-

Table 1. Compositions and Thermal Behavior of the PIB/ASD IPN Samples

Samples[a]	Composition (Wt Ratio)	T_d (°C)[b]
PIB	PIB/ASD(100/0)	348.6
PIB90	PIB/ASD(90/10)	293.3
PIB70	PIB/ASD(70/30)	272.0
PIB50	PIB/ASD(50/50)	276.4
PIB30	PIB/ASD(30/70)	278.5
PIB10	PIB/ASD(10/90)	282.7
ASD	PIB/ASD(0/100)	247.2

[a]Samples were cured at 180°C for 2 hours.
[b]T_d was read at the temperature corresponding to 5% wt. loss.

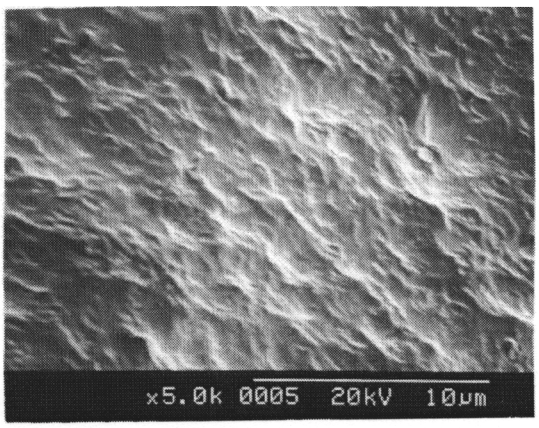

(a)

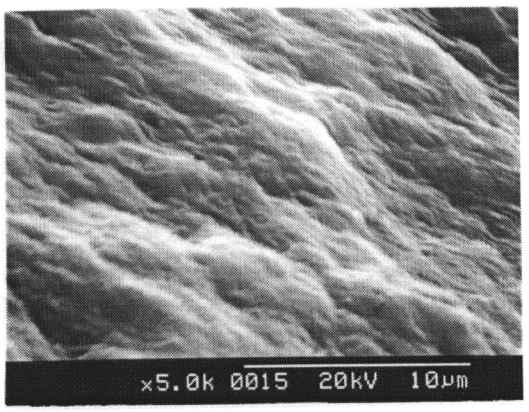

(b)

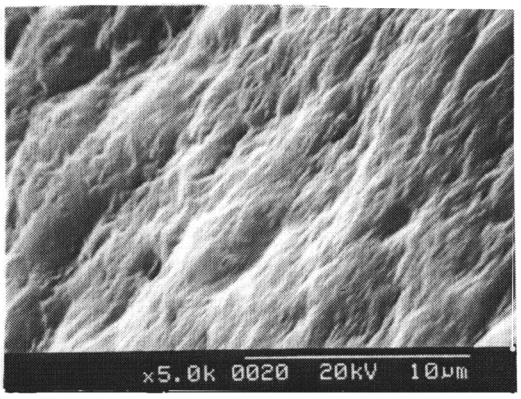

(c)

Figure 5. Scanning electron micrographs of the cured (a) PIB90, (b) PIB50, and (c) PIB10 samples.

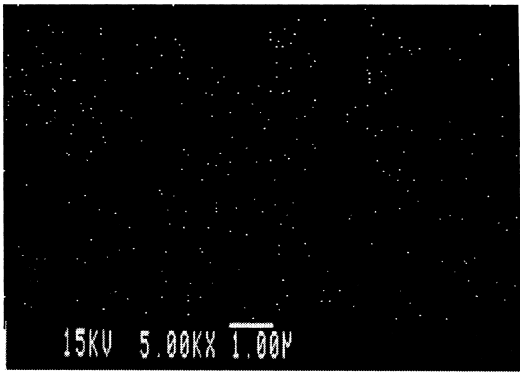

(a)

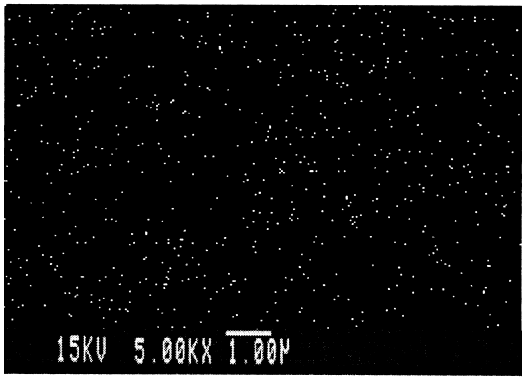

(b)

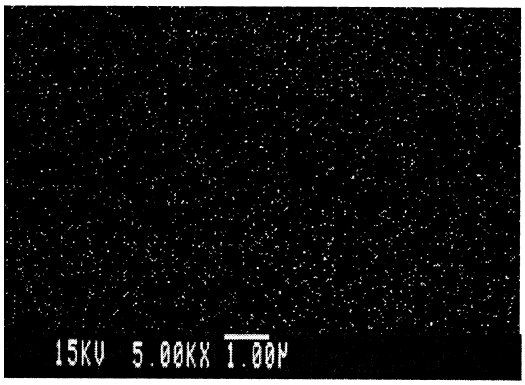

(c)

Figure 6. SEM mapping micrographs of the cured (a) PIB90, (b) PIB50, and (c) PIB10 samples.

cate that the silicons are distributed uniformly throughout the polymer film. Moreover, the silica particle sizes are much smaller than 1 μm for these samples because of their total transparency as examined by UV-vis transmission spectra [28].

The time dependence of the absorption behavior is shown in Figure 7 for the PIB50 IPN sample. The absorption spectrum was taken regularly over 170 hour period under thermal treatment at 100°C. The maximum of the absorption was located around 470 nm. Immediately after poling/curing, a decrease in absorption and a blue shift were observed in the spectrum. This was due to dichroism and electrochromism resulting from the induced dipole alignment [29]. During the next 170 hours, the absorption spectrum remained unchanged. This demonstrated that the orientation of the poled chromophores was not relaxed significantly after thermal treatment. The absorption behavior of the PIB50 IPN sample is similar to that of the poled/cured PIA50 sample [20].

The linear optical properties of these NLO sol-gel materials are summarized in Table 2. Thicknesses of the polymer films are between 0.8 and 1.9 μm. The refraction indices are ranged from 1.60 to 1.76, and increase with increasing content of ASD. Second-harmonic coefficients d_{33} and d_{31} of poled/cured ASD, and PIB/ASD samples at 1064 nm are summarized in Table 3. These PIB/ASD IPN samples exhibit large second-order nonlinearity. Moreover, the second-harmonic

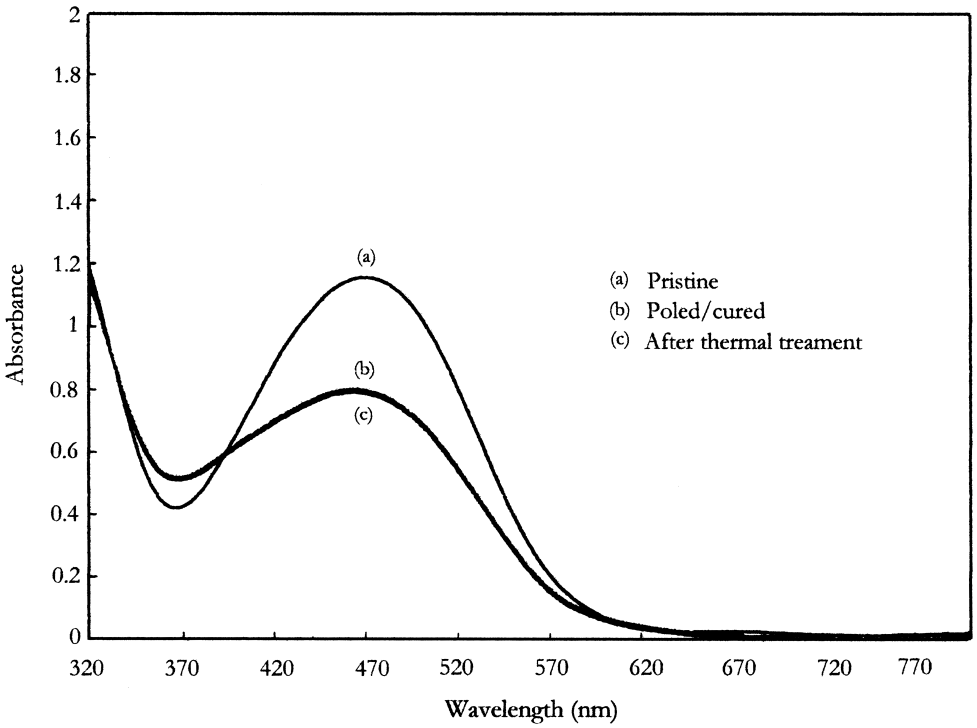

Figure 7. UV/vis absorption spectra of the PIB50 sample.

Table 2. Thicknesses and Refraction Indices of the PIB/ASD IPN Samples

Samples	d(μm)[a]	n_{543}[b]	n_{633}	n_{830}
ASD	1.1	1.72	1.68	1.65
PIB10	1.2	1.76	1.74	1.73
PIB30	1.5	1.75	1.74	1.73
PIB50	1.9	1.69	1.64	1.63
PIB70	1.1	1.64	1.63	1.60
PIB90	0.8	1.69	1.66	1.65

[a]d = the thickness of polymer film.
[b]n_{543}, n_{633}, n_{830} = refraction indices at 543, 633, and 830 nm, respectively.

coefficients increase with increasing content of ASD. A similar result was also observed for the poled/cured PIA/ASD samples [20]. In addition, the temporal characteristics of the second harmonic coefficients for the poled/cured ASD and PIB/ASD samples at 100°C are shown in Figure 8. A much better temporal stability was obtained for the PIB/ASD IPN samples as compared with the poled/cured ASD. The temporal stability was increased with decreasing content of ASD. Figure 9 shows dynamic NLO stability of the PIB50 IPN sample. By extrapolation of slow and fast relaxations of the effective second harmonic coefficients, the T_0 (210°C) was found. This T_0 is 20 degree higher than that of the poled/cured PIA/ASD sample with the same ASD content [20]. Moreover, the PIB/ASD IPN samples also exhibit better temporal stability than the poled/cured PIA/ASD samples [20]. This indicates that the entanglements between different networks of IPN system are effective to restrict the mobility of the aligned NLO chromophores.

The dynamic NLO thermal stability of the poled/cured PIA/ASD and PIB/ASD samples was studied at different temperatures. Decay of the second harmonic coefficient is described by the Kohlrausch-Williams-Watts function (KWW) for the poled/cured samples [30]

$$d_{33}(t)/d_{33}(0) = \exp^{-(t/\tau)\beta}$$

Table 3. Second Harmonic Coefficients d_{33} and d_{31} (pm/V) of the PIB/ASD IPN Samples at 1064 nm

Samples	$d_{33(1064)}$	$d_{31(1064)}$
ASD	54.0	19.2
PIB10	39.6	15.7
PIB30	30.3	12.5
PIB50	22.5	7.5
PIB70	10.8	3.9
PIB90	6.9	3.1

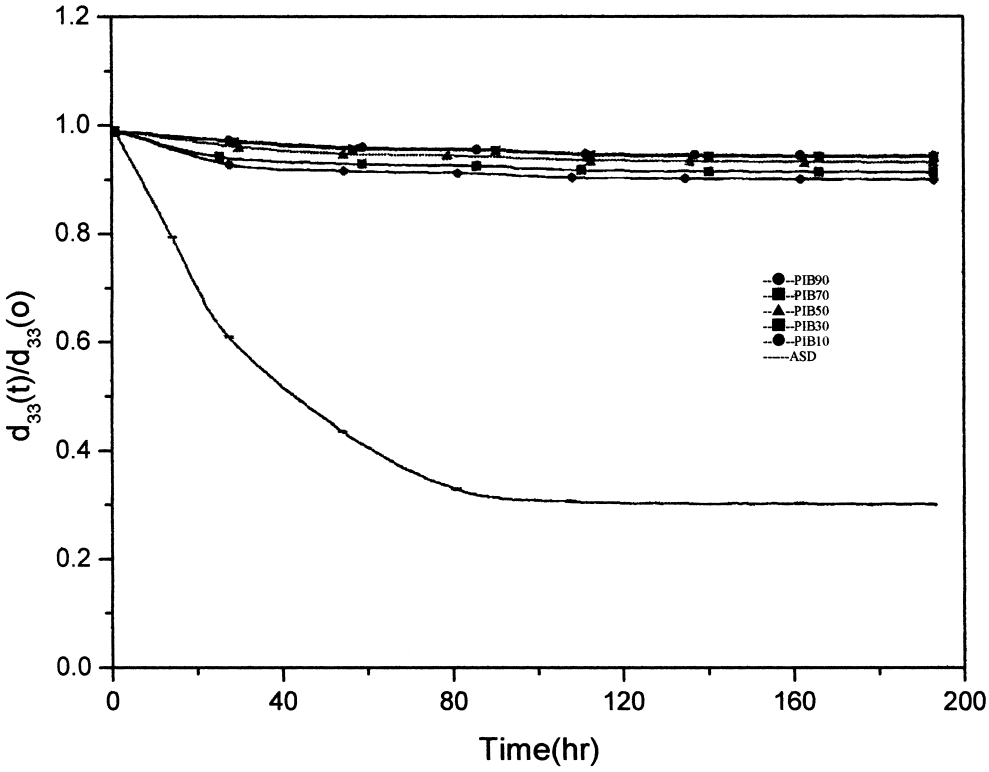

Figure 8. Temporal behavior of the second harmonic coefficient for the PIB/ASD IPN samples at 100°C.

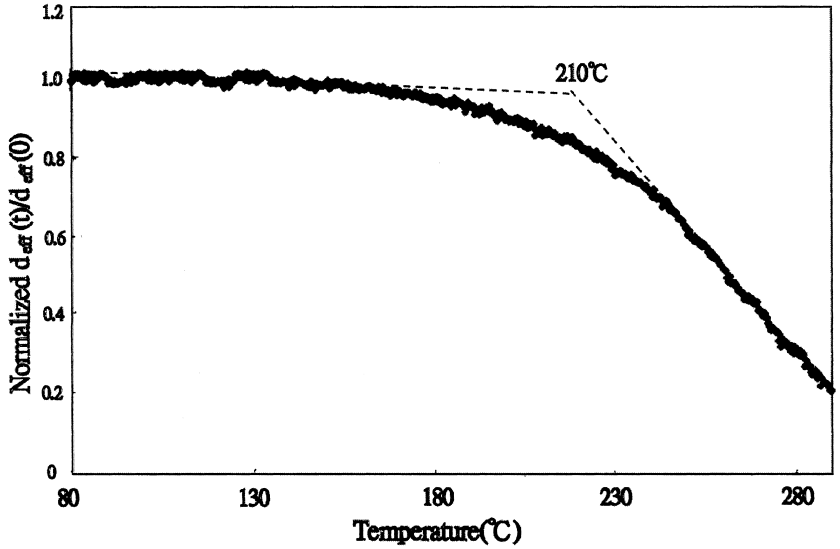

Figure 9. Temperature dependence of the dipole re-orientational dynamics of the PIB50 IPN sample.

where τ represents the relaxation time, and broadening parameter β is a constant between 0 and 1, which characterizes the parameter of the relaxation time distribution. The composition effect on the relaxation time of the poled/cured PIA/ASD and PIB/ASD samples is shown in Figure 10. The relaxation time was increased with increasing content of polyimide. Higher temperatures resulted in fast decay of second harmonic coefficient, which possessed a shorter relaxation time for the poled/cured polyimides/ASD samples. Moreover, the PIB/ASD IPN samples exhibited much longer relaxation times than the poled/cured PIA/ASD samples. In addition, the composition effect on the value of the broadening parameter is shown in Figure 11 for the poled/cured polyimide/ASD samples. The value of the

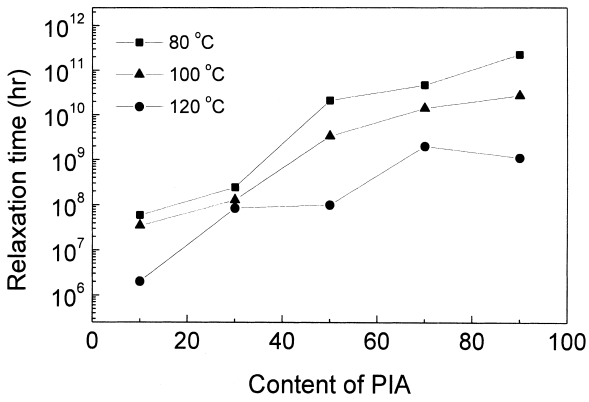

(a)

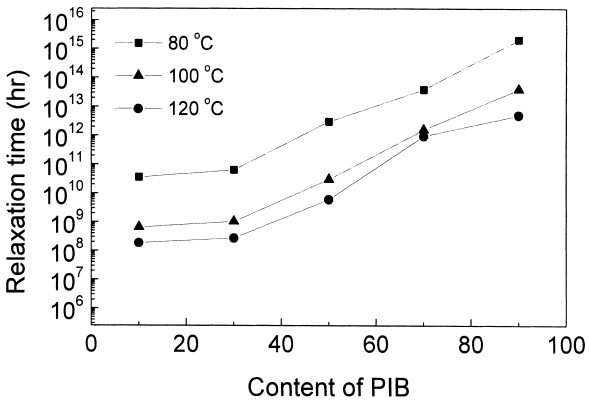

(b)

Figure 10. Relaxation time versus polyimide content for the poled/cured (a) PIA/ASD, and (b) PIB/ASD samples at different temperatures.

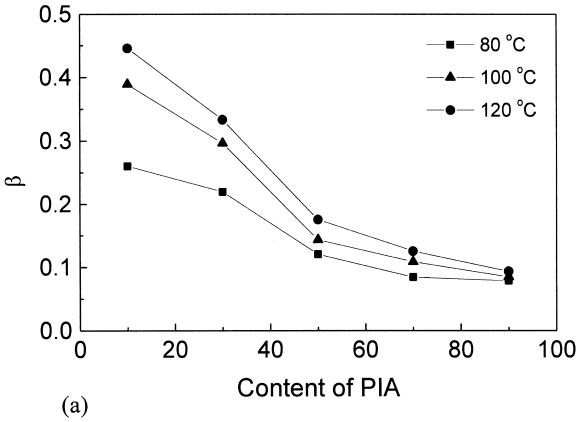

(a)

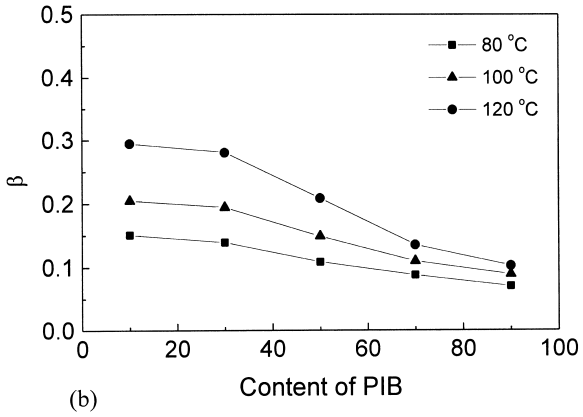

(b)

Figure 11. Broadening parameter versus polyimide content for the poled/cured (a) PIA/ASD, and (b) PIB/ASD samples at different temperatures.

broadening parameter was increased with increasing content of ASD due to the fact that the NLO chromophores were more easily to be poled under the electric filed for the sample with a lower T_g and a higher ASD content. Higher poling efficiency resulted in a higher degree of uniform alignment of the NLO chromophores, which exhibited a narrower distribution of the relaxation time. Moreover, the poled/cured PIA/ASD samples exhibited larger values of β than the poled/cured PIB/ASD samples. This indicates that the surrounding of NLO chromophores in the PIB/ASD IPN samples is more inhomogeneous than the interchain crosslinking system of PIA/ASD samples. In addition, an increase in the broadening parameter as a function of temperature reflects a gradual narrowing distribution of the relaxation time. As the temperature increases, the molecular mobility of the each NLO chromophore reaches the same level, which results in the gradual narrowing distribution of the relaxation time [31].

CONCLUSION

A series of the NLO polyimide/inorganic interpenetrating polymer networks have been developed. Large second-order nonlinearity (d_{33} = 6.9-39.6 pm/V) was obtained after the poling/curing process. The entanglements between different networks of IPN system was more efficient to restricting the mobility of the aligned NLO chromophores than that of the inter-chain crosslinking polyimide/inorganic system [20]. Consequently, the PIB/ASD IPN samples exhibited a much better temporal stability than the poled inter-chain crosslinked PIA/ASD samples. Much longer relaxation time and smaller value of broadening parameter were obtained for the IPN samples as compared with the poled/cured PIA/ASD samples.

ACKNOWLEDGMENT

This paper is dedicated to R. J. Jeng's beloved teacher, Professor Sukant Tripathy. Financial support from National Science Council of Taiwan, ROC (Grant NSC89-2216-E-005-002) is acknowledged.

REFERENCES

1. Prasad, P.N.; Williams, D.J. In *Introduction to Nonlinear Optical Effects in Molecules and Polymers*; John Wiley & Sons, Inc.: New York, 1991.
2. Singer, K.D; Sohn, J.E.; Lalama, S.J. Appl. Phys. Lett., **1986**, *49*, 248.
3. Meredith, G.R.; Dusen, J G.; Williams, D.J. Macromolecules **1982**, *15*, 1385.
4. Wang, N.P.; Leslie, T.M.; Wang, S.; Kowel, S.T. Chem. Mater. **1995**, *7*, 185.
5. Stenger-Smith, J.D.; Henry, R.A.; Hoover, J.M.; Lindsay, G.A.; Nadler, M.P.; Nissan, R.A. J. Polym. Sci. **1993**, *31*, 2899.
6. Xu, C.; Wu, B.; Todorova, O.; Dalton, L.R.; Shi, Y.; Ranon, P.M.; Steier, W.H. Macromolecules **1993**, *26*, 5303.
7. Jeng, R.J.; Chen, Y.M.; Jain, A.; Tripathy, S.K.; Kuman, J. Optics Commun. **1992**, *89*, 212.
8. Kim, J.; Plawsky, J.L.; LaPeruta, R.; Korenowski, G.M. Chem. Mater. **1992**, *4*, 249.
9. Jeng, R.J.; Chen, Y.M.; Chen, J.I.; Kumar, J.; Tripathy, S.K. Macromolecules **1993**, 26, 2530.
10. Marturunkakul, S.; Chen, J.I.; Jeng, R.J.; Sengupta, S.; Kumar, J.; Tripathy, S.K. Chem. Mater. **1993**, *5*, 743.
11. Wu, J.W.; Valley, J.F.; Ermer, S.; Binkley, E.S.; Kenney, J.T.; Lipscomb, G.F.; Lytel, R. Appl. Phys. Lett. **1991**, *58*, 225.
12. Jeng, R.J.; Chen, Y.M.; Jain, A.K.; Kumar, J.; Tripathy, S.K. Chem. Mater. **1992**, *4*, 1141.
13. Lin, J.T.; Hubbard, M.A.; Marks, T.J.; Lin, W.; Wong, G.K. Chem. Mater. **1992**, *4*, 1148.
14. Hsiue, G.H.; Kuo, J.K.; Jeng, R.J. Chem. Mater. **1994**, *6*, 884.
15. Jeng, R.J.; Chen, Y.M.; Jain, A.; Tripathy, S.K.; Kuman, J. Optics Commun. **1992**, 89, 212.

16. Claude, C.; Garetz, B.; Okamoto, Y.S.; Tripathy, K. Mater. Lett., **1992**, *14*, 336.
17. Oviatt, H.W.; Shea, K.J.; Kalluri, S.; Shi, Y.; Steier, W.H.; Dalton, L.R. Chem. Mater. **1995**, *7*, 493.
18. Kim, J.; Plawsky, J.L.; LaPeruta, R.; Korenowski, G.M.; Chem. Mater. **1992**, *4*, 249.
19. Landry, C.J.T.; Coltrain, B.K.; Wesson, J.A.; Zumbulyadis, N.; Lippert, J.L. Polymer **1992**, *33*, 1496.
20. Jeng, R.J.; Chan, L.H.; Lee, R.H. Journ. Mac. Sci.: Pure & Appl. Chem. Submitted.
21. Marturunkakul, S.; Chen, J.I.; Li, L.; Jeng, R.J.; Kumar, J.; Tripathy, S.K. Chem. Mater. **1993**, *5*, 592.
22. Lakshmanan, P.; Srinivasan, S.; Moy, T.; McGrath, J.E. Polym. Prepr. Am. Chem. Soc., Div. Polym. Chem. **1993**, *34*, 707.
23. Mandal, B.; Jeng, R.J.; Kumar, J.; Tripathy, S.K. Makromol. Chem., Rapid Commun. **1991**, *12*, 607.
24. Mortazavi, M.A.; Knoesen; A.; Kowel, S.T.; Higgins, B.G.; Dienes, A. J. Opt. Soc. Am. **1989**, *B6*, 773.
25. Jeng, R.J.; Chen, Y.M.; Kumar, J.; Tripathy, S.K. Journ. Mac. Sci., Pure & Appl. Chem. **1992**, *A29*, 1115.
26. Mandal, B.K.; Chen, Y.M.; Lee, J.Y.; Kumar, J.; S.K. Tripathy, Appl. Phys. Lett. **1991**, *58*, 2459.
27. Wung, C.J.; Lee, K.S.; Prasad, P.N.; Kim, J.C.; Jin, J.I.; Shim, H.K. Polymer **1992**, *33*, 4145.
28. Wen, J.; Dhandapani, B.S.; Oyama, T.; Wilkes, G.L. Chem. Mater. **1997**, *9*, 1968.
29. Yang, Z.; Xu, C.; Wu, B.; Dalton, L.R.; Kalluri, S.; Steier, W.H.; Shi, Y.; Bechtel, J.H. Chem. Mater. **1994**, *6*, 1899.
30. Firestone, M.A.; Ratner, M. A.; Marks, T.J. Macromolecules **1995**, *28*, 6296.
31. Bristow, J.F.; Kalika, D.S.; Macromolecules **1994**, *27*, 1808.